



Fláajökull (north lobe), Iceland: active temperate piedmont lobe glacial landsystem

Journal:	<i>Journal of Maps</i>
Manuscript ID:	TJOM-2015-0092.R1
Manuscript Type:	Original Article
Date Submitted by the Author:	13-Jul-2015
Complete List of Authors:	Evans, David,John,Alexander; University of Durham, Geography Ewertowski, Marek; Durham University, Geography; Adam Mickiewicz University, Faculty of Geographical and Geological Sciences Orton, Chris; Durham University, Department of Geography
Keywords:	glacial landsystem, active temperate glacier, Iceland

SCHOLARONE™
Manuscripts

1
2
3
4
5
6
7
8
9
10
11
12
13
14
15
16
17
18
19
20
21
22
23
24
25
26
27
28
29
30
31
32
33
34
35
36
37
38
39
40
41
42
43
44
45
46
47
48
49
50
51
52
53
54
55
56
57
58
59
60

1 Fláajökull (north lobe), Iceland: active temperate piedmont lobe
2 glacial landsystem

3 David J A Evans, Marek Ewertowski and Chris Orton

4 Department of Geography, Durham University, South Road, Durham DH1 3LE, UK

5 Corresponding author: d.j.a.evans@durham.ac.uk

6

For Peer Review Only

7

8 Abstract

9 A 1:6,250 map of the foreland of Fláajökull's north lobe as it appeared in 1989, together with a 1:350
10 scale map of a sample area of recently exposed glacial landforms from 2014, enables an assessment
11 of the spatial and temporal evolution of glacial landform assemblages at the margin of an active
12 temperate piedmont lobe terminating at ice-marginal thickening till wedges. The pattern of
13 landform development captured in these maps indicates that the glacier margin developed strong
14 longitudinal crevassing and well-developed ice-marginal pecten (three dimensional crenulations)
15 during its historical recession. This is recorded by early recessional phase linear push moraines on
16 well-drained distal slopes of the foreland and the later development of inter-related sawtooth
17 moraines, crevasse squeeze ridges and till eskers, indicative of extending ice flow and poorly drained
18 sub-marginal conditions. This landform record is a palaeoglaciological signature of a changing
19 process-form regime inherent within the active temperate piedmont lobe landsystem model.

20 Key words: glacial landsystem; active temperate glacier; Iceland

21

22 1. Introduction

23 The aim of this study was to map, at the large scale of 1:6,250, the distribution of glacial sediment-
24 landform associations on the Fláajökull north lobe foreland (Figure 1), an area that displays a
25 conspicuous arcuate moraine assemblage, comprising fluted/overridden ridges, recessional push
26 ridges and geometrical ridge networks. This landsystem signature displays many similarities to that
27 of the neighbouring forelands of Heinabergsjökull and Skálafellsjökull (Evans & Orton 2014),
28 indicative of all these glacier snouts being characterized by the dynamics of active temperate
29 piedmont lobes. However, the density of overridden moraines and widespread occurrence of
30 sawtooth moraines (cf. Price 1970; Matthews et al. 1979; Fredin & Burki 2008; Burki et al. 2009) with
31 unusually long limbs, geometrical ridges (crevasse infills), and numerous till eskers (*sensu*
32 Christoffersen et al. 2005; Larsen et al. 2006; Evans et al. 2010) are embellishments specific to this
33 landsystem that reflect the intensive development of longitudinal crevassing in lobate snouts
34 terminating at marginal-thickening till wedges (cf. Evans & Hiemstra 2005) rather than outwash
35 heads, as exemplified at Heinabergsjökull. Given the importance of the juxtaposition and complex
36 interactions of the various sub-marginal landforms evolving at the glacier snout at the present day, a
37 further larger scale map (1:350) was produced for a small area of the foreland based upon an
38 unmanned aerial vehicle (UAV) aerial survey in 2014. This large scale mapping provides some details

1
2
3 39 representative of the complex set of landforms that have emerged on the foreland since 1989,
4 40 during which time Fláajökull has receded by more than 500 m

5
6 41

7 42 **2. Methods of map production**

8
9
10 43 The map 1:6,250 map has been produced with no new topographical ground survey of the study
11 44 area. Hence the landform and surficial geology mapping was undertaken on two, non-rectified, and
12 45 manually stitched aerial photographs taken by Landmælingar Íslands in 1989, and contours are
13 46 derived from the existing 1:50,000 topographic map, based on the ISN 93 datum. The relief of most
14 47 landforms is less than the 20 m contour intervals and therefore the lack of newly surveyed contours
15 48 does not impact significantly on the representation of the glacial geomorphology. The distortion
16 49 inherent in non-rectified aerial photographs was minimized by using the central portions of the
17 50 images for mapping. The glacier surface is represented by a mask compiled directly from the aerial
18 51 photographs but does not contain any contours as these were not surveyed for this map.
19
20
21
22
23
24
25

26 53 Since 1989 Fláajökull has receded by more than 500 m along most of its margin, exposing a complex
27 54 network of glacial landforms. Continued observations on the spatial and temporal development of
28 55 these landforms provide invaluable insights into the evolution of the glacial geomorphology of the
29 56 whole foreland and hence a large scale (1: 350) map of the most recent features exposed at the
30 57 north side of the snout was compiled based on a UAV survey in September 2014 (Figure 2). Low
31 58 altitude images were taken using a small, lightweight UAV quadcopter equipped with a 12-
32 59 megapixel, wide-angle lens camera. Images were acquired at an elevation of 40 m above the
33 60 launching point. The ground image pixel size was ~0.016 m. In total four flights were performed and
34 61 175 images were taken covering 0.1 km². The craft was equipped with a 3D gimbal system and
35 62 because images were acquired while the craft was hovering, photographs were all well focussed.
36 63 The images were handled with Agisoft Photoscan software. A point-cloud containing 98.90 million
37 64 points was generated and subsequently georeferenced to the UTM 28N coordinate system using 23
38 65 ground control points (GCPs). GCPs were surveyed with Topcon Hiper II dGPS system and post-
39 66 processed. GCPs were used to optimize and provide survey control on the point-cloud. An average
40 67 density of points was 963.7 points/m². Finally, meshed 3D models were generated from the point-
41 68 cloud and subsequently transformed into a raster, grid DEM with 0.03 m cell size. The total DEM
42 69 error measured against GCPs was 0.063 m (x = 0.037, y = 0.038, z = 0.035). A low-density point-cloud
43 70 was used to produce an orthophoto mosaic with the 0.016 m cell size to enable high resolution
44 71 landform mapping.
45
46
47
48
49
50
51
52
53
54
55
56
57
58
59
60

73 3. Historical evolution of the Fláajökull snout and foreland

74 The earliest map of Fláajökull is the Danish Geodetic Survey map of 1904, which depicts the glacier
75 margin some 300 m inside the maximum historical limit (Figure 1). Evans et al. (1999)
76 lichenometrically dated the outermost moraine of Fláajökull's south lobe, in the valley (Heinar) that
77 joins the foreland of Heinabergsjökull. From this they proposed an age of 1884/85 based upon the
78 age-size approach and an acceptance of historical documentation that indicates an 1887 AD
79 maximum age for the outermost Little Ice Age moraines in the area, for both Heinabergsjökull and
80 Fláajökull (Thorarinsson 1939); the period 1882-1892 was identified by Ahlmann and Thorarinsson
81 (1937) as a time frame for the maximum of the most recent Little Ice Age advance of Fláajökull. A
82 longer chronology has been proposed by McKinzey et al. (2004, 2005) for the Heinabergsjökull
83 moraines lying immediately inside the proposed 1887 AD moraines of Evans et al. (1999). This is
84 based upon the employment of the size-frequency lichenometric method and the discovery of
85 tephras in the moraine stratigraphy, suggesting a date of sometime between 1850 and 1887 AD,
86 using Bradwell's (2004) age-gradient curve, or 1818–1886 AD, using Bradwell's (2001) age-size curve.
87 These calculations infer an older age for Evans et al.' (1999) outer moraine, a moraine that Dabski
88 (2002, 2007) suggests dates to 1870-1894 AD using a variety of dating methods and archives.

89
90 In the early to mid-1990s, a number of south Vatnajökull outlet glaciers, including Fláajökull,
91 readvanced and maintained a quasi-stationary ice front for around 5 years (cf. Bradwell et al. 2006;
92 Evans et al. 2009; Bennett & Evans 2012). This was significant in terms of the Fláajökull foreland
93 geomorphology in that it resulted in the construction of a composite push moraine (Evans 2003,
94 2005; Evans & Hiemstra 2005) typical of stationary temperate glacier snouts (Krüger 1993; Evans
95 2013). This moraine was being initiated at the time of aerial photograph capture in 1989 and was
96 observed during its construction and abandonment over the period 1993-2002, allowing a full
97 understanding of the process-form relationships and process sedimentology associated with sub-
98 marginal till accretion and moraine genesis (Evans & Hiemstra 2005).

99 The large lakes that are portrayed on the map near the snout have been deepened and extended by
100 the artificial damming of the westerly flowing meltwater rivers as part of a long term strategy to
101 divert the proglacial drainage over the sandur (see "made ground" surficial geology classification).
102 More recently, further dams have been constructed to divert the majority of the drainage again
103 towards the west, resulting in the more extensive flooding of the landforms portrayed on this map
104 around the large lakes and in the linear sandur corridors that are aligned ice margin parallel.

105 4. Glacial geomorphology and surficial geology

106 Seven surficial geology map units are identified on the glacier foreland on the 1:6,250 scale map,
107 each one being associated with specific landforms and geomorphic process-form regimes. These are
108 colour-coded on the map and relevant landforms are depicted using symbology, following the
109 protocol established for previous Icelandic glacier foreland maps (Bennett et al. 2010; Evans & Twigg
110 2002; Evans et al. 2006a, 2007, 2009; Evans & Orton 2014; Howarth & Welch 1969a, 1969b). The
111 foreland is dominated by glacial fluvial deposits and till, with other surficial units forming only minor
112 coverage.

114 4.1 Till and moraine

115 The till and moraines surficial map unit is characterized by the surface flutings and recessional push
116 moraines typical of the active temperate landsystems of southern Iceland but also contains
117 conspicuous crevasse fill ridges and minor till eskers, that are not widely displayed in active
118 temperate forelands elsewhere. Individual till stratigraphic units are typically less than 1 m thick and
119 display all the characteristics of subglacial traction till (Evans 2000; Evans et al. 2006b). Thicker till
120 coverage occurs where composite moraines have been constructed by marginal till wedge stacking,
121 resulting in repeating vertical sequences of multiple A and B horizons (*sensu* Boulton & Hindmarsh
122 1987; Figure 3). Such a process was observed during the early 1990s, when a negative North Atlantic
123 Oscillation signal triggered glacier snout readvance and stabilization for at least 5 years (Bradwell et
124 al. 2006; Evans & Hiemstra 2005; Figure 4a, b). The resulting composite moraine (Figure 4c) was
125 under construction on the 1989 aerial photographs and hence is depicted in this map at the glacier
126 margin. Thicker tills also occur where the most recent (historical Little Ice Age) till sheet overlies
127 overridden moraines. More common are thin tills (<1 m thick) and individual recessional push
128 moraines, which are produced every year and typically have a saw-tooth or crenulated plan form
129 (Figure 5). This morphology has been clearly related in Iceland to construction along glacier snouts
130 strongly indented by closely spaced, longitudinal crevasses or pecten (Price 1970; Sharp 1984; Evans
131 & Twigg 2002; Evans & Orton 2014). The localized close spacing of these moraines, together with
132 annual shifts in the positioning of pecten, gives rise to areas of extremely complex superimposition
133 (Figure 5). Although the fine-grained diamictic till blanket and sawtooth push moraines dominate the
134 till and moraine map unit, more bouldery tills and moraines have been constructed at the former
135 southwest margin of the glacier (Figure 6). Here a sequence of marginally stacked boulder-rich tills
136 have been constructed at the historical Little Ice Age maximum limit, documenting the delivery of
137 coarser debris loads to the former ice margin from the steep bedrock bluffs that separate the north
138 and south lobes of Fláajökull.

1
2
3 139
4
5 140 The locally well-developed crevasse fill ridges and minor till eskers are morphologically distinct from
6
7 141 push moraines because they are orientated oblique to push moraine crests but not parallel to
8
9 142 former ice flow, the latter indicated by adjacent fluting patterns. The crevasse fill ridges are similar
10
11 143 to the geometric ridge networks described from many other glacier forelands (cf. Sharp 1985; Evans
12
13 144 & Rea 1999, 2003; Jónsson et al. 2014) in that they comprise numerous straight limbs attached end
14
15 145 on end, and in places cross each other to form elongate rectilinear nets. However, they nowhere
16
17 146 resemble the dense, polygonal net shapes that have been reported as evidence of surge-induced
18
19 147 crevasse squeeze ridge construction in Iceland (Sharp 1985; Evans & Rea 1999; Kjær et al. 2008; Rea
20
21 148 & Evans 2011; Schomacker et al. 2014). In a number of cases these ridges merge into, or are aligned
22
23 149 with, the limbs of sawtooth moraines, indicating that they originated by a similar depositional
24
25 150 mechanism. Many such examples are now visible on the recently (post 1990s) deglaciated foreland
26
27 151 (Figure 7), some of which are difficult to distinguish from flutings because they have been squeezed
28
29 152 up into very long longitudinal crevasses. Hence the Fláajökull crevasse fill ridges are a product of
30
31 153 glacier sub-marginal till squeezing into the dense longitudinal crevasse networks that give rise to
32
33 154 remarkably indented radial pecten at the snout. Therefore the sawtooth push moraines and
34
35 155 crevasse fill ridges are a landform assemblage diagnostic of strong radial ice flow in piedmont lobes
36
37 156 overlying deforming till in saturated (poorly drained) locations (cf. Jónsson et al. 2014). Their
38
39 157 predominance on the tops of overridden moraine arcs on only the inner half of the foreland attests
40
41 158 to the former extensional crevassing created in the ice margin by the localized, arcuate topographic
42
43 159 high points in the glacier bed.

37 160
38
39 161 Sinuous diamicton ridges or till eskers (Figure 8) have been identified previously on only a few glacier
40
41 162 snouts globally (cf. Christoffersen et al. 2005; Larsen et al. 2006; Evans et al. 2010). Their origin in
42
43 163 Icelandic settings is hypothesized to relate to the squeezing of dilatant till into an elongated cavity or
44
45 164 R-channel immediately after meltwater evacuation, during a short period when the pressure
46
47 165 gradient between the cavity and the till bed was steep and hence saturated till was subject to
48
49 166 localized creep towards the elongate low pressure zone (Evans et al. 2010). In order to be preserved
50
51 167 on a deglaciated foreland, till eskers must have been produced during the final stages of subglacial
52
53 168 sedimentation, otherwise shear deformation would have remoulded them. As crevasse squeeze
54
55 169 ridge preservation requires the same conditions, it is unsurprising to find them juxtaposed with till
56
57 170 eskers (Figure 9).

55 171

1
2
3 172 Previous maps of the forelands of Icelandic active temperate glaciers have depicted areas of discrete
4 173 overridden moraines but the extensive nature of the overridden moraine arcs at Fláajökull
5 174 necessitate their inclusion in the till and moraine mapping unit. They constitute the underlying
6 175 topography of the till and moraine area but are most prominent in the middle and inner foreland
7 176 where they give rise to enclosed contours at 40 m and 60 m above sea level (Figure 10). They are
8 177 inset, low amplitude arcs of fluted till (cf. Evans et al. 1999, 2009; Evans & Orton 2014; Evans &
9 178 Twigg 2002; Krúger 1994) deposited prior to or during glacier advance to the historical Little Ice Age
10 179 limit and then superimposed by sharper relief recessional push moraines during snout recession. The
11 180 crests of the more recent push moraines are predominantly orientated parallel with the summit
12 181 crests of the overridden moraines, making them easy to distinguish from other adornments
13 182 including crevasse fill ridges and till eskers. Areas dominated by overridden moraines are evident
14 183 also on the map where elongate ponds are absent or rare; such ponds are common between the
15 184 localized high points formed by the recessional push moraines, especially on the outer foreland
16 185 where overridden moraine arcs are less prominent.
17
18
19
20
21
22
23
24
25
26

27 187 **4.2 Glacifluvial deposits**

28 188 Glacifluvial deposits (including sand and gravel-cored eskers) are predominantly located in proglacial
29 189 outwash sandur fans and glacier-margin parallel linear sandar. The major terraces and eroded cliffs
30 190 on the sandar are mapped by the identification of terrace and cliff edges. The sandur fans, occupying
31 191 the southwest, south and east parts of the map, were constructed largely during the historical Little
32 192 Ice Age maximum when proglacial streams drained the outermost moraine arc. These have been
33 193 incised and are now only partially occupied by the modern drainage after it passes through corridors
34 194 between the overridden moraine arcs. Recent attempts by farmers to modify the drainage have
35 195 given rise to localized ponding of these drainage corridors. The corridors are occupied by linear
36 196 sandar which are orientated parallel to the ice-margin because they have been and are directed by
37 197 the underlying topography of the overridden moraine arcs (Figure 10). Sand and gravel cored eskers
38 198 are rare on the foreland, being located only in a large melt-out depression on the north side of the
39 199 snout. This depression and its associated landforms, including the eskers, has evolved and gradually
40 200 drained over the last two decades. The evolution of the area from a largely flat but locally pitted
41 201 outwash surface to a large depression containing gravel and sand mounds and esker ridges displays
42 202 all the process-form relationships of areas of melting glacier snouts buried by glacifluvial outwash
43 203 and containing englacial drainage tunnels. Similar landform assemblages have evolved at the
44 204 margins of Breiðamerkurjökull (Evans & Twigg 2002), Kviárjökull (Bennett et al. 2010; Bennett &
45
46
47
48
49
50
51
52
53
54
55
56
57
58
59
60

205 Evans 2012) and Virkisjökull/Falljökull (Livingstone et al. 2010; Bradwell et al. 2013), where
206 meltwater drainage appears to have bypassed overdeepenings in the subglacial environment.

207 **4.3 Glacilacustrine deposits**

208 A minor pocket of glacilacustrine deposits occurs on the northern part of the foreland, where it
209 records the gradual emptying of the large melt-out depression produced by burying of part of the
210 glacier snout by glacifluvial outwash. This forms a thin blanket to a veneer generally less than 3 m
211 thick of sands, silts and clays.

213 **4.4 Bedrock, residuum and paraglacial deposits**

214 Minor surficial units of bedrock, residuum and paraglacial deposits are depicted at the western and
215 northern extremities of the map where they occur in association with the steep mountain slopes of
216 Jökulfell and Fláafjall respectively. The *in situ* weathering products of the bedrock, which occur on the
217 more shallow slopes and knolls, are classified as residuum. These areas of weathered bedrock also
218 contain small patches of deeply weathered or wind deflated pre-Little Ice Age till too small to depict
219 at this scale. Also present in such areas are localized drapes of aeolian (tephra) deposits and peat,
220 especially in topographic hollows, again too small for representation at this scale. The paraglacial
221 deposits include colluvial and debris flow fed fans reworked since historical glacier recession from
222 glacial deposits on steeper slopes. Also included as paraglacial materials are scree slopes and debris
223 flow fans derived from mechanically weathered bedrock outcrops. Numerous small bedrock
224 outcrops, too small to map at this scale, also occur within the areas mapped as paraglacial deposits.

226 **4.5 Made ground**

227 Due to the localized historical modification of the foreland by farmers attempting to divert glacial
228 meltwater, there are small areas of made ground. These constitute dams which have also been used
229 as tracks and occur only in the western part of the foreland.

231 **Spatial and temporal changes in the Fláajökull foreland: implications for the active temperate 232 glacial landsystem model**

233 Glacial landsystem maps allow the identification of landform patterns which can be instructive in
234 relating process to form in both a spatial and temporal framework (cf. Bennett et al. 2010; Evans &
235 Twigg 2002;). At Fláajökull, the north lobe has produced a distinct set of landform patterns that can
236 be related to changing glaciological conditions through time and hence allow us to refine the active
237 temperate piedmont lobe landsystem model (Figure 11). Firstly, we interpret the multiple arcs of
238 overridden moraines as products of composite push ridge construction during phases of glacier

1
2
3 239 stillstand (cf. Evans & Hiemstra 2005), either during a previous period of snout recession or during its
4 240 advance to the Little Ice Age maximum. The marked snout-parallel linearity of the sandar deposited
5 241 since recession from the Little Ice Age maximum limit has been developed as a result of the
6 242 topographic control exerted by the overridden moraine arcs. Secondly, the recessional push
7 243 moraines display two clear patterns; closely spaced and more linear forms occur on the outer
8 244 foreland, whereas more sawtooth and partially superimposed forms occur on the inner foreland.
9 245 The moraines of the inner foreland are also arranged in a series of clusters, the spacing between
10 246 each cluster getting progressively smaller towards the present glacier margin. These two zones are
11 247 separated by a fluted till surface with very few, fragmented push moraines, recording a period of
12 248 glacier retreat over a distance of 250 m when moraine construction was subdued, likely due to rapid
13 249 snout recession. Prior to and after this, more substantial push moraines were constructed every 2-50
14 250 m, with some superimposed moraines indicating several or more years of ice marginal stillstand.
15 251 Finally, the distribution of crevasse squeeze ridges and till eskers on the inner foreland indicates that
16 252 sub-marginal conditions were conducive to the squeezing of till into full depth crevasses and tunnels
17 253 in the snout during the more recent period of glacier recession. This coincides with the change in
18 254 push moraine pattern identified above and therefore represents a geomorphic signature of a change
19 255 from a non-crevassed to a longitudinally crevassed snout with well-developed pecten as well as a
20 256 change from a well-drained to poorly-drained foreland.

21
22
23
24
25
26
27
28
29
30
31
32
33 257 The underlying control on both of these inter-related changes is the topography of the substrate
34 258 that was inherited by the glacier snout as it advanced and retreated from its historical Little Ice Age
35 259 maximum. Specifically this topography was the surface of the overridden moraine arcs, as defined by
36 260 the enclosed 40 m and 60 m contours; these contours define two overridden moraine arcs, the
37 261 outermost of which possesses a long, shallow distal slope on which the outer zone of linear
38 262 recessional push moraines and flutings are developed. The inner zone of superimposed sawtooth
39 263 moraines, crevasse squeeze ridges and till eskers are developed inside the steeper, proximal slope of
40 264 the outer overridden moraine arc; the increased spacing density of the sawtooth moraines begins
41 265 inside the innermost overridden moraine arc where more extensive areas of low lying, poorly
42 266 drained surfaces occur. Since 1989, when the aerial photographs used for mapping were taken,
43 267 another overridden moraine arc has emerged, as represented by the enclosed 60 m contours on the
44 268 northeast side of snout; this topographic high point has been adorned with the composite push
45 269 moraine constructed during the mid-1990s readvance (Figure 5). Hence the glacial geomorphology
46 270 records the development of strong longitudinal crevassing and concomitant well-developed ice-
47 271 marginal pecten in the north lobe during its historical recession (Figure 9); during early recession
48 272 from the shallow distal slope of the outermost overridden moraine, ice flow was most likely

1
2
3 273 compressive and hence the ice margin was not heavily crevassed. Drainage was also unimpeded
4 274 towards the south and onto the proglacial sandur fan. In contrast, since recession from the steeper
5 275 proximal slope of the outermost overridden moraine arc, ice flow has been extensional as well as
6 276 strongly lobate and the glacier snout has progressively thinned. Therefore full depth crevassing and
7 277 pecten production has been the dominant control on glacier sub-marginal and marginal landform
8 278 construction. Combined with the relatively poor proglacial drainage imparted by the emerging
9 279 subglacial topography, this has given rise to a clear change in the nature and distribution of glacial
10 280 landforms on the foreland and hence a palaeoglaciological signature of a changing process-form
11 281 regime in an active temperate glacier lobe fed by marginal-thickening till wedges.

18 282 **Conclusion**

20 283 The 1:6,250 scale map of the glacial geomorphology and surficial geology of the Fláajökull north lobe
21 284 foreland depicts an arcuate moraine assemblage, composed of fluted and overridden moraines
22 285 superimposed by smaller recessional push moraines, geometrical ridge networks (crevasse squeeze
23 286 ridges) and till eskers. The overridden moraines contain cores of multiple tills and associated
24 287 glaciifluvial sediments and mark the locations of former composite push moraine construction by
25 288 glacier-marginal till thickening during periods of glacier stillstand, similar to that observed during the
26 289 mid-1990s. They were overridden and fluted by the glacier during its advance to the Little Ice Age
27 290 maximum and, despite being superimposed by smaller scale recessional landforms, their
28 291 morphology has exerted a topographic control on the routing of proglacial outwash in snout-parallel
29 292 linear sandar tracts. This subglacial topography, comprising three inset overridden moraine arcs lying
30 293 inside a shallow distal sloping foreland, has been influential also in changing the glaciological and
31 294 sub-marginal drainage conditions through time, as documented by the nature and pattern of the
32 295 superimposed landforms that document the historical recession of the snout. The landforms indicate
33 296 that the piedmont glacier lobe developed strong longitudinal crevassing and well-developed ice-
34 297 marginal pecten during its historical recession. This is recorded by early recessional phase linear
35 298 push moraines on the shallow, well-drained distal slope of the outermost overridden moraine,
36 299 indicative of compressive ice flow, followed by later development of inter-related sawtooth
37 300 moraines, crevasse squeeze ridges and till eskers, indicative of extending ice flow and poorly drained
38 301 sub-marginal conditions. Hence the glacial geomorphology of the Fláajökull north lobe foreland
39 302 documents a clear palaeoglaciological signature of a changing process-form regime and allows us to
40 303 refine the active temperate piedmont lobe landsystem model, specific to forelands characterized by
41 304 marginal-thickening till wedges and the topographic influence these wedges impose on smaller scale
42 305 landform production in relation to glacier snout crevasse networks and sub-marginal drainage

306 conditions. It also clearly demonstrates that the holistic nature of the landsystems mapping
307 approach is a powerful tool in deciphering the palaeoglaciological record.

308

309 **Software**

310 The dGPS ground control points were processed using the Canadian Spatial Reference System (CSRS)
311 Precise Point Positioning (PPP) tool. The orthophotomap and digital elevation model from UAV-
312 based images were produced in Agisoft Photoscan Professional Edition. The geomorphology for the
313 1:350 map was prepared in ESRI ArcGIS and edited in Adobe Illustrator. The 1:6,250 scale map was
314 drawn in Adobe Illustrator and the glacier image manipulation was undertaken in Adobe Photoshop.

315

316 **References**

- 317 Ahlmann, H.W., & Thorarinsson, S. (1937). Previous investigations of Vatnajökull: marginal
318 oscillations of its outlet glaciers and general description of its morphology. *Geografiska*
319 *Annaler*, 19A, 176-211.
- 320 Bennett, G. L., & Evans, D. J. A. (2012). Glacier retreat and landform production on an overdeepened
321 glacier foreland: The debris-charged glacial landsystem at Kvíárjökull, Iceland. *Earth Surface*
322 *Processes and Landforms*, 37, 1584–1602.
- 323 Bennett, G. L., Evans, D. J. A., Carbonneau, P., & Twigg, D. R. (2010). Evolution of a debris-charged
324 glacier landsystem, Kvíárjökull, Iceland. *Journal of Maps*, 2010, 40–76.
- 325 Boulton, G.S., & Hindmarsh, R.C.A. (1987). Sediment deformation beneath glaciers: rheology and
326 geological consequences. *Journal of Geophysical Research*, 92, 9059–9082.
- 327 Bradwell, T. (2001). A new lichenometric dating curve for southeast Iceland. *Geografiska Annaler*,
328 83A, 91–101.
- 329 Bradwell, T. (2004). Lichenometric dating in southeast Iceland – The size-frequency approach.
330 *Geografiska Annaler*, 86A, 31–41.
- 331 Bradwell, T., Dugmore, A.J., Sugden, D.E. (2006). The Little Ice Age glacier maximum in Iceland and
332 the North Atlantic Oscillation: evidence from Lambatungnajökull, southeast Iceland. *Boreas*,
333 35, 61–80.
- 334 Bradwell, T., Sigurðsson, O., & Everest, J. (2013). Recent, very rapid retreat of a temperate glacier in
335 SE Iceland. *Boreas* 42, 959-973.
- 336 Burki, V., Larsen, E., Fredin, O., & Margreth, A. (2009) The formation of sawtooth moraine ridges in
337 Bødalen, western Norway. *Geomorphology*, 105, 182-192.
- 338 Christoffersen, P., Piotrowski, J.A., & Larsen, N.K. (2005). Basal processes beneath an Arctic glacier
339 and their geomorphic imprint after a surge, Elisebreen, Svalbard. *Quaternary Research* 64,
340 125–137.
- 341 Dabski, M. (2002) Dating of the Fláajökull moraine ridges, SE Iceland: comparison of the glaciological,
342 cartographic and lichenometrical data. *Jökull* 51, 17-24.
- 343 Dabski, M. (2007). Testing the size-frequency based lichenometric dating curve on Fláajökull

- 1
2
3 344 moraines (SE Iceland) and quantifying lichen population dynamics with respect to stone
4 345 surface aspect. *Jökull*, 57, 21-35.
- 5 346 Evans, D. J. A. (2000). A gravel outwash/deformation till continuum, Skálafellsjökull, Iceland.
6 347 *Geografiska Annaler*, 82A, 499–512.
- 8 348 Evans, D. J. A. (2003). Ice-marginal terrestrial landsystems: Active temperate glacier margins. In D. J. A.
9 349 Evans (Ed.), *Glacial landsystems* (pp. 12–43). London: Arnold.
- 10 350 Evans, D. J. A. (2005). The glacier-marginal landsystems of Iceland. In C. J. Caseldine, A. J. Russell,
11 351 J. Harðardóttir, & Ó. Knudsen (Eds.), *Iceland: Modern processes and past environments* (pp.
12 352 93–126). Amsterdam: Elsevier.
- 14 353 Evans, D. J. A. (2013). The glacial and periglacial research – Geomorphology and retreating glaciers.
15 354 In J. Shroder (Editor in Chief), R. Giardino, J. Harbor (Eds.), *Treatise on geomorphology*.
16 355 Academic Press, San Diego, CA, vol. 8, *Glacial and Periglacial Geomorphology*, pp. 460–478.
- 18 356 Evans, D.J.A., & Orton, C. (2014) Heinabergsjökull and Skálafellsjökull, Iceland: active temperate
19 357 piedmont lobe and outwash head glacial landsystem. *Journal of Maps*, 2014
20 358 <http://dx.doi.org/10.1080/17445647.2014.919617>
- 22 359 Evans, D.J.A., Archer, S., & Wilson, D.J.H. (1999). A comparison of the lichenometric and Schmidt
23 360 hammer dating techniques based on data from the proglacial areas of some Icelandic
24 361 glaciers. *Quaternary Science Reviews*, 18, 13–41.
- 26 362 Evans, D.J.A., & Hiemstra, J.F. (2005). Till deposition by glacier submarginal, incremental thickening.
27 363 *Earth Surface Processes and Landforms* 30, 1633–1662.
- 28 364 Evans, D.J.A., Nelson, C.D., & Webb, C. (2010). An assessment of fluting and “till eskers” formation on
29 365 the foreland of Sandfellsjökull, Iceland. *Geomorphology* 114, 453-465.
- 30 366 Evans, D. J. A., Phillips, E. R., Hiemstra, J. F., & Auton, C. A. (2006b). Subglacial till: Formation,
31 367 Sedimentary characteristics and classification. *Earth Science Reviews*, 78, 115–176.
- 33 368 Evans, D. J. A., & Rea, B.R. (1999). The geomorphology and sedimentology of surging glaciers: A land-
34 369 systems approach, *Annals of Glaciology*, 28, 75–82.
- 36 370 Evans, D. J. A., Shand, M., & Petrie, G. (2009). Maps of the snout and proglacial landforms of
37 371 Fjallsjökull, Iceland (1945, 1965, 1998). *Scottish Geographical Journal*, 125, 304–320.
- 38 372 Evans, D. J. A., & Twigg, D. R. (2002). The active temperate glacial landsystem: A model based on
39 373 Breiðamerkurjökull and Fjallsjökull, Iceland. *Quaternary Science Reviews*, 21, 2143–2177.
- 40 374 Evans, D. J. A., Twigg, D. R., Rea, B. R., & Shand, M. (2007). Surficial geology and geomorphology of
41 375 the Bruarjökull surging glacier landsystem. *Journal of Maps*, 3, 349–367.
- 43 376 Evans, D. J. A., Twigg, D. R., & Shand, M. (2006a). Surficial geology and geomorphology of the
44 377 Þorísjökull plateau icefield, west-central Iceland. *Journal of Maps*, 2, 17–29.
- 45 378 Fredin, O., & Burki, V. (2008). A photogrammetric digital elevation model of
46 379 the Bødalen valley saw-tooth moraine complex, western Norway. *Journal of Maps*, 2008, 63-
47 380 70.
- 48 381 Howarth, P. J., & Welch, R. (1969a). Breiðamerkurjökull, South-east Iceland, August 1945. 1:30,000
49 382 scale map, University of Glasgow.
- 51 383 Howarth, P. J., & Welch, R. (1969b). Breiðamerkurjökull, South-east Iceland, August 1965. 1:30,000
52 384 scale map, University of Glasgow.
- 53 385 Jónsson, S.A., Schomacker, A., Benediktsson, Í.Ö., Ingólfsson, Ó., & Johnson, M.D. (2014). The
54 386 drumlin field and the geomorphology of the Múlajökull surge-type glacier, central Iceland.
55 387 *Geomorphology*, 207, 213-220.
- 57 388 Kjær, K.H., Korsgaard, N.J., & Schomacker, A. (2008). Impact of multiple glacier surges – a

- 389 geomorphological map from Brúarjökull, east Iceland. *Journal of Maps*, 2008, 5-20.
- 390 Krüger, J. (1993). Moraine-ridge formation along a stationary ice front in Iceland. *Boreas*, 22, 101–
- 391 109.
- 392 Krüger, J. (1994). Glacial processes, sediments, landforms and stratigraphy in the terminus region of
- 393 Mýrdalsjökull, Iceland. *Folia Geographica Danica*, 21, 1–233.
- 394 Larsen, N.K., Piotrowski, J.A., Christoffersen, P., & Menzies, J. (2006). Formation and deformation of
- 395 basal till during a glacier surge; Elisebreen, Svalbard. *Geomorphology* 81, 217–234.
- 396 Livingstone, S.J., Evans, D.J.A., Ó Cofaigh, C., & Hopkins, J. (2010). The Brampton Kame Belt and
- 397 Pennine Escarpment Meltwater Channel System (Cumbria, UK). *Morphology, Sedimentology*
- 398 *and Formation. Proceedings of the Geologists' Association*, 121, 423–443.
- 399 Matthews, J.A., Cornish, R., & Shakesby, R.A. (1979). "Saw-tooth" moraines in front of
- 400 Bødalsbreen, southern Norway. *Journal of Glaciology*, 88, 535–546.
- 401 McKinzey, K. M., Orwin, J. F., & Bradwell, T. (2004). Re-dating the moraines at Skálafellsjökull and
- 402 Heinabergsjökull using different lichenometric methods: Implications for the timing of the
- 403 Icelandic Little Ice Age maximum. *Geografiska Annaler*, 86A, 319–335.
- 404 McKinzey, K. M., Orwin, J. F., & Bradwell, T. (2005). A revised chronology of key Vatnajökull (Iceland)
- 405 outlet glaciers during the Little Ice Age. *Annals of Glaciology*, 42, 171–179.
- 406 Price, R. J. (1970). Moraines at Fjallsjökull, Iceland. *Arctic and Alpine Research*, 2, 27–42.
- 407 Rea, B.R., & Evans, D.J.A. (2011). An assessment of surge-induced crevassing and the formation of
- 408 crevasse squeeze ridges. *Journal of Geophysical Research*, 116, F04005,
- 409 Doi:10.1029/2011jf001970, 2011.
- 410 Schomacker, A., Benediktsson, Í.Ö., & Ingólfsson, Ó. (2014). The Eyjabakkajökull glacial landsystem,
- 411 Iceland: geomorphic impact of multiple surges. *Geomorphology*, 218, 98-107.
- 412 Sharp, M. J. (1984). Annual moraine ridges at Skálafellsjökull, south-east Iceland. *Journal of*
- 413 *Glaciology*, 30, 82–93.
- 414 Sharp, M. J. (1985). "Crevasse-fill" ridges: A landform type characteristic of surging glaciers?
- 415 *Geografiska Annaler*, 67A, 213–220.
- 416 Thorarinsson, S. (1939). The ice dammed lakes of Iceland with particular reference to their values as
- 417 indicators of glacial oscillation. *Geografiska Annaler*, 21, 216–242.

420 **Figure captions**

421 Figure 1: Annotated Google Earth image of Fláajökull and its foreland, showing the positions of the

422 glacier snout through time based on various records.

424 Figure 2: Workflow diagram showing the construction of the 1:350 scale map of a portion of the

425 recently deglaciated foreland based on UAV captured imagery.

427 Figure 3: Stratigraphic exposure through the innermost overridden moraine arc on the north side of

428 the foreland, with boundaries between major sedimentary units marked by dashed lines. The lowest

429 unit in the cliff is glacialfluvial outwash and this is overlain by multiple tills with minor and

430 discontinuous lenses of sand and gravel. Note that minor push moraines lie on the surface of the

431 overridden ridge and these are related to the uppermost till.

1
2
3 433 Figure 4: The early to mid-1990s composite push moraine: a) during formation on the central
4 434 foreland in 1993; b) cross section through the moraine on the north foreland after its abandonment
5 435 in 2002, with multiple till units identified (after Evans & Hiemstra 2005); c) view across the moraine
6 436 on the west foreland in 2014. Note the very steep distal and proximal slopes at this location.
7 437

8 438 Figure 5: View across the north foreland in 2008, showing the early to mid-1990s composite moraine
9 439 in the centre foreground and the cross-cutting nature of this and the earlier sawtooth moraines as
10 440 well as the most recent deglaciated foreland with its complex of overprinted push moraines,
11 441 crevasse squeeze ridges and till eskers.
12 442

13 443 Figure 6: The historical Little Ice Age maximum moraines on the southwest margin of the north lobe:
14 444 a) view across the moraine ridges, showing their bouldery nature; b) stratigraphic exposure through
15 445 the moraines, showing glacier marginally stacked boulder-rich tills outlined by dashed lines.
16 446

17 447 Figure 7: View across the recently deglaciated foreland in 2014, showing the details of cross-cutting
18 448 and merging of crevasse squeeze ridges, sawtooth moraine limbs and frontal lobes, and minor
19 449 flutings. The dense longitudinal crevasse networks and pecten responsible for these landforms are
20 450 visible in the glacier snout.
21 451

22 452 Figure 8: Sinuous diamicton ridge, interpreted as a till esker, on the central foreland.
23 453

24 454 Figure 9: Views across the recently deglaciated foreland showing the juxtaposition of crevasse
25 455 squeeze ridges/sawtooth moraines and sparse till eskers, including the area surveyed for the 1:350
26 456 scale map: a) ground view with main landforms identified; b) UAV oblique aerial photograph looking
27 457 south; c) UAV oblique aerial photograph looking north, towards the glacier snout and showing the
28 458 relationship between landform orientations and pecten.
29 459

30 460 Figure 10: View across an overridden moraine arc and linear, ice margin-parallel sandur towards the
31 461 historical Little Ice Age maximum limit. The overridden moraine is outlined by the dashed line and is
32 462 covered by crevasse squeeze ridges and minor flutings as well as some small recessional push
33 463 moraines.
34 464

35 465 Figure 11: Conceptual model for the spatial and temporal development of the landform assemblages
36 466 on the Fláajökull north lobe foreland, along a simplified topographical cross profile from the
37 467 historical Little Ice Age limit to the present glacier margin.
38 468
39 469

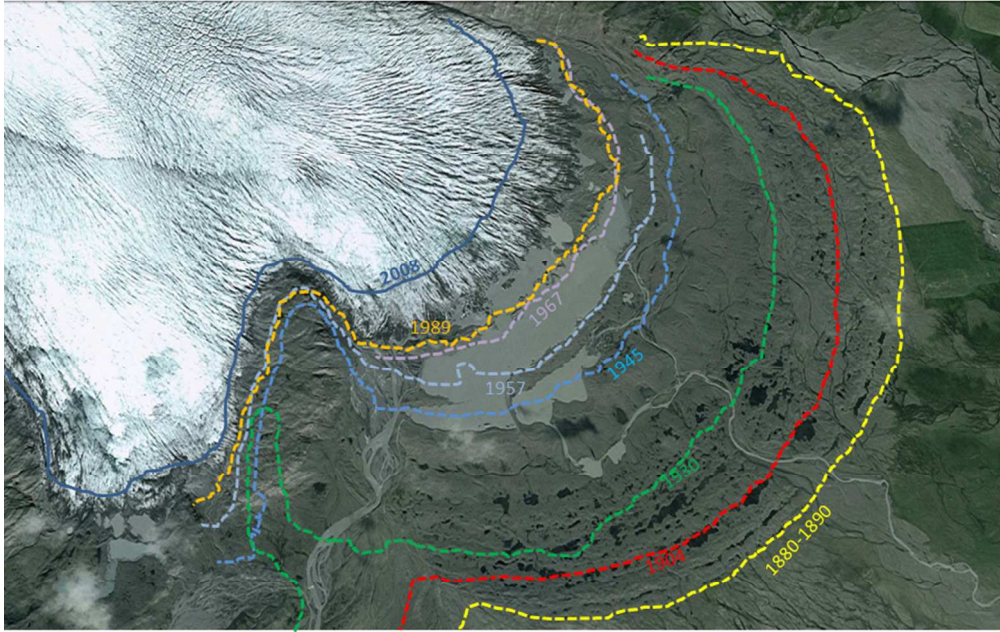
470 **Acknowledgements**

471 Fieldwork at Fláajökull has been conducted during a number of field seasons under the auspices of
472 the University of Glasgow Iceland Expeditions 1993 and 2002, and the Durham University Iceland
473 Expeditions 2009 and 2014, funded by the Royal Scottish Geographical Society, Carnegie Trust and
474 Royal Geographical Society. ME was supported by a Marie Curie Intra European Fellowship, 7th 471
475 Framework Programme (REA agreement number 299130). Comments by reviewers Simon Carr,
476 Richard Waller, Alan Kehew and Anders Schomacker helped us to clarify the contents of this paper.

477

For Peer Review Only

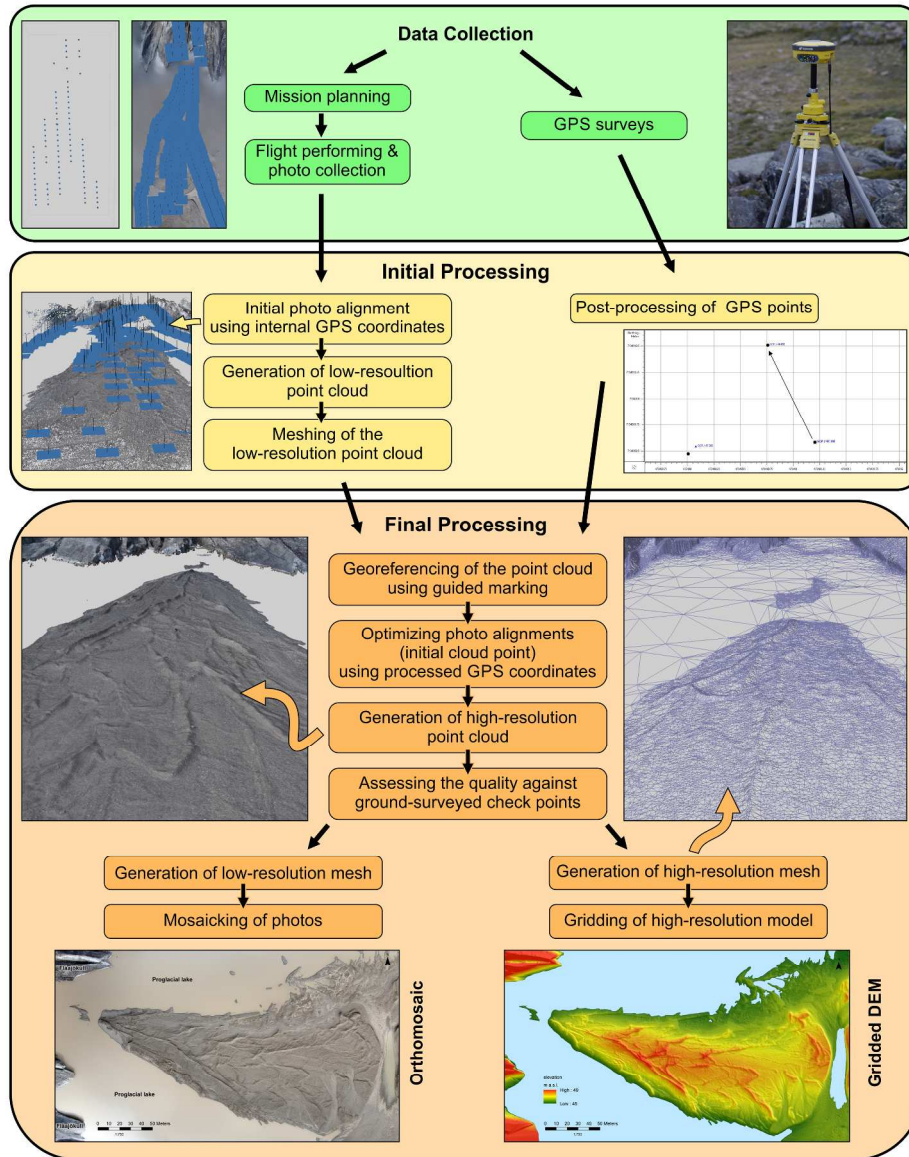
1
2
3
4
5
6
7
8
9
10
11
12
13
14
15
16
17
18
19
20
21
22
23
24
25
26
27
28
29
30
31
32
33
34
35
36
37
38
39
40
41
42
43
44
45
46
47
48
49
50
51
52
53
54
55
56
57
58
59
60



254x190mm (96 x 96 DPI)

View Only

1
2
3
4
5
6
7
8
9
10
11
12
13
14
15
16
17
18
19
20
21
22
23
24
25
26
27
28
29
30
31
32
33
34
35
36
37
38
39
40
41
42
43
44
45
46
47
48
49
50
51
52
53
54
55
56
57
58
59
60



250x313mm (300 x 300 DPI)

1
2
3
4
5
6
7
8
9
10
11
12
13
14
15
16
17
18
19
20
21
22
23
24
25
26
27
28
29
30
31
32
33
34
35
36
37
38
39
40
41
42
43
44
45
46
47
48
49
50
51
52
53
54
55
56
57
58
59
60



254x190mm (96 x 96 DPI)

View Only

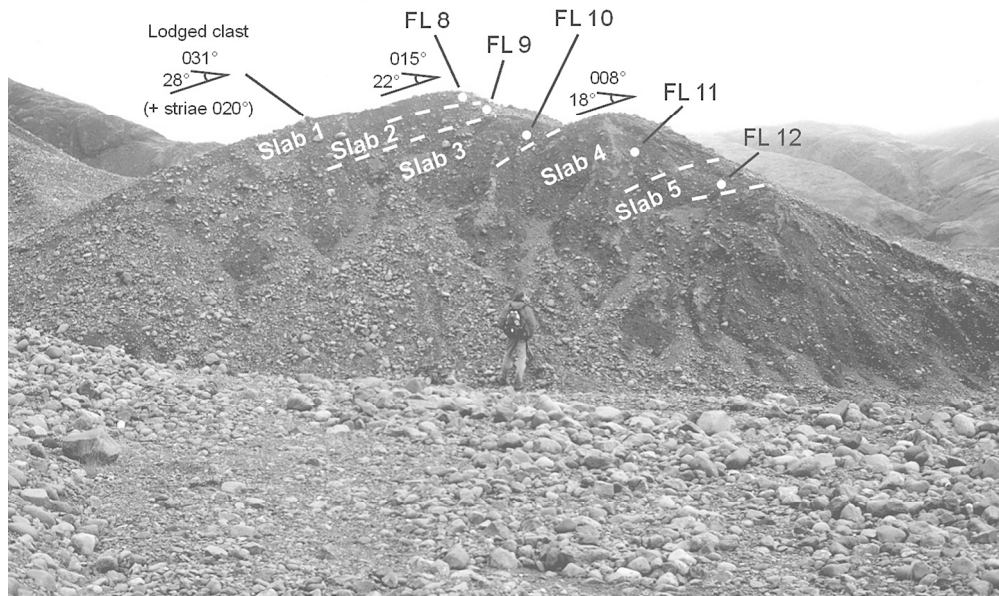
1
2
3
4
5
6
7
8
9
10
11
12
13
14
15
16
17
18
19
20
21
22
23
24
25
26
27
28
29
30
31
32
33
34
35
36
37
38
39
40
41
42
43
44
45
46
47
48
49
50
51
52
53
54
55
56
57
58
59
60



22x15mm (600 x 600 DPI)

Review Only

1
2
3
4
5
6
7
8
9
10
11
12
13
14
15
16
17
18
19
20
21
22
23
24
25
26
27
28
29
30
31
32
33
34
35
36
37
38
39
40
41
42
43
44
45
46
47
48
49
50
51
52
53
54
55
56
57
58
59
60



119x81mm (300 x 300 DPI)

Review Only

1
2
3
4
5
6
7
8
9
10
11
12
13
14
15
16
17
18
19
20
21
22
23
24
25
26
27
28
29
30
31
32
33
34
35
36
37
38
39
40
41
42
43
44
45
46
47
48
49
50
51
52
53
54
55
56
57
58
59
60



823x229mm (300 x 300 DPI)

Peer Review Only

1
2
3
4
5
6
7
8
9
10
11
12
13
14
15
16
17
18
19
20
21
22
23
24
25
26
27
28
29
30
31
32
33
34
35
36
37
38
39
40
41
42
43
44
45
46
47
48
49
50
51
52
53
54
55
56
57
58
59
60



254x190mm (96 x 96 DPI)

View Only

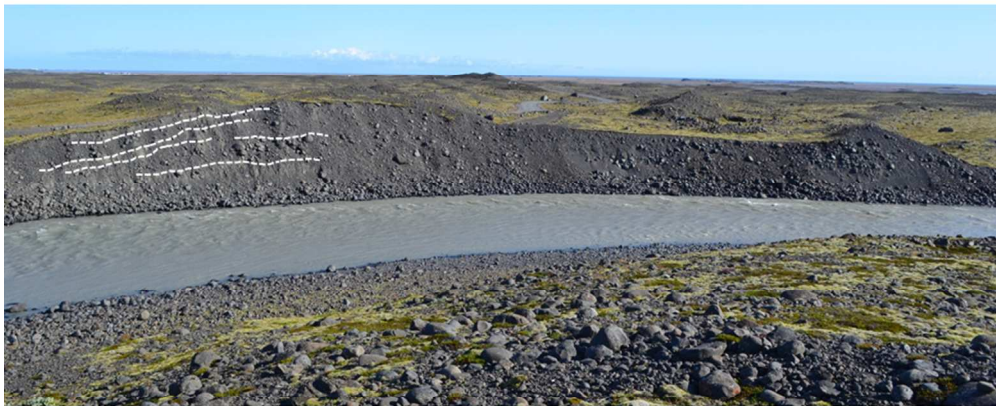
1
2
3
4
5
6
7
8
9
10
11
12
13
14
15
16
17
18
19
20
21
22
23
24
25
26
27
28
29
30
31
32
33
34
35
36
37
38
39
40
41
42
43
44
45
46
47
48
49
50
51
52
53
54
55
56
57
58
59
60



869x244mm (300 x 300 DPI)

Peer Review Only

1
2
3
4
5
6
7
8
9
10
11
12
13
14
15
16
17
18
19
20
21
22
23
24
25
26
27
28
29
30
31
32
33
34
35
36
37
38
39
40
41
42
43
44
45
46
47
48
49
50
51
52
53
54
55
56
57
58
59
60



254x190mm (96 x 96 DPI)

View Only

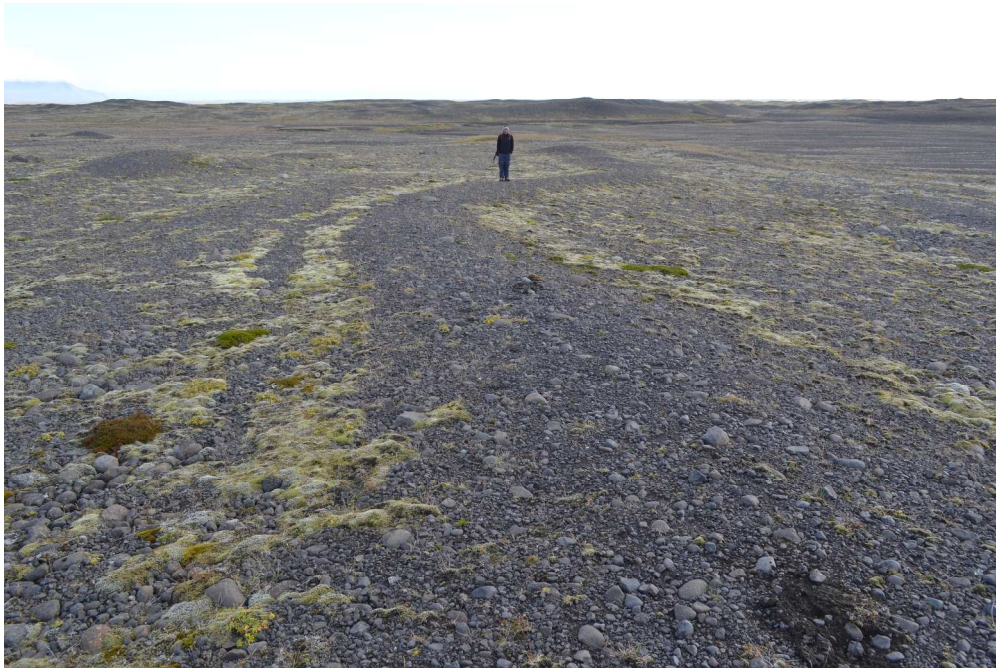
1
2
3
4
5
6
7
8
9
10
11
12
13
14
15
16
17
18
19
20
21
22
23
24
25
26
27
28
29
30
31
32
33
34
35
36
37
38
39
40
41
42
43
44
45
46
47
48
49
50
51
52
53
54
55
56
57
58
59
60



556x251mm (300 x 300 DPI)

er Review Only

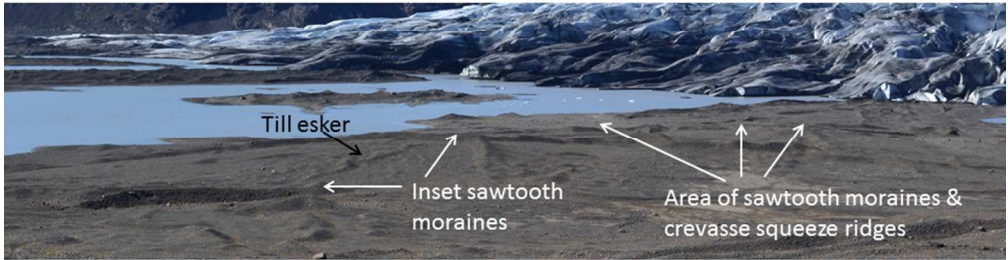
1
2
3
4
5
6
7
8
9
10
11
12
13
14
15
16
17
18
19
20
21
22
23
24
25
26
27
28
29
30
31
32
33
34
35
36
37
38
39
40
41
42
43
44
45
46
47
48
49
50
51
52
53
54
55
56
57
58
59
60



390x260mm (300 x 300 DPI)

Review Only

1
2
3
4
5
6
7
8
9
10
11
12
13
14
15
16
17
18
19
20
21
22
23
24
25
26
27
28
29
30
31
32
33
34
35
36
37
38
39
40
41
42
43
44
45
46
47
48
49
50
51
52
53
54
55
56
57
58
59
60



254x190mm (96 x 96 DPI)

View Only

1
2
3
4
5
6
7
8
9
10
11
12
13
14
15
16
17
18
19
20
21
22
23
24
25
26
27
28
29
30
31
32
33
34
35
36
37
38
39
40
41
42
43
44
45
46
47
48
49
50
51
52
53
54
55
56
57
58
59
60



463x347mm (240 x 240 DPI)

View Only

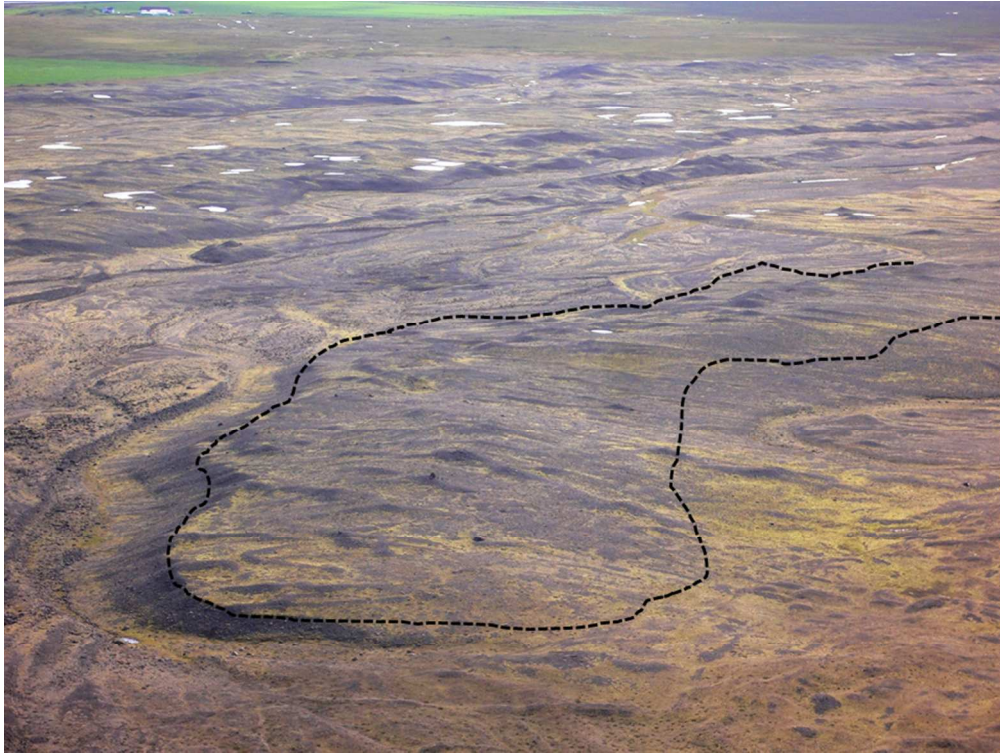
1
2
3
4
5
6
7
8
9
10
11
12
13
14
15
16
17
18
19
20
21
22
23
24
25
26
27
28
29
30
31
32
33
34
35
36
37
38
39
40
41
42
43
44
45
46
47
48
49
50
51
52
53
54
55
56
57
58
59
60



463x347mm (240 x 240 DPI)

View Only

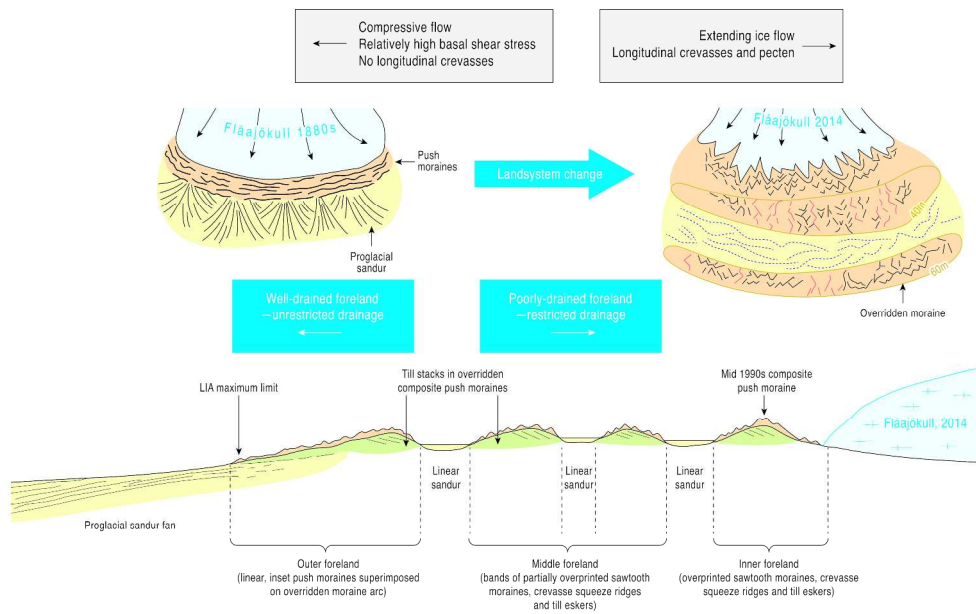
1
2
3
4
5
6
7
8
9
10
11
12
13
14
15
16
17
18
19
20
21
22
23
24
25
26
27
28
29
30
31
32
33
34
35
36
37
38
39
40
41
42
43
44
45
46
47
48
49
50
51
52
53
54
55
56
57
58
59
60



254x190mm (96 x 96 DPI)

View Only

1
2
3
4
5
6
7
8
9
10
11
12
13
14
15
16
17
18
19
20
21
22
23
24
25
26
27
28
29
30
31
32
33
34
35
36
37
38
39
40
41
42
43
44
45
46
47
48
49
50
51
52
53
54
55
56
57
58
59
60



279x178mm (300 x 300 DPI)

Review Only

473000

474000

475000

476000

7135000

7134000

7133000

7132000

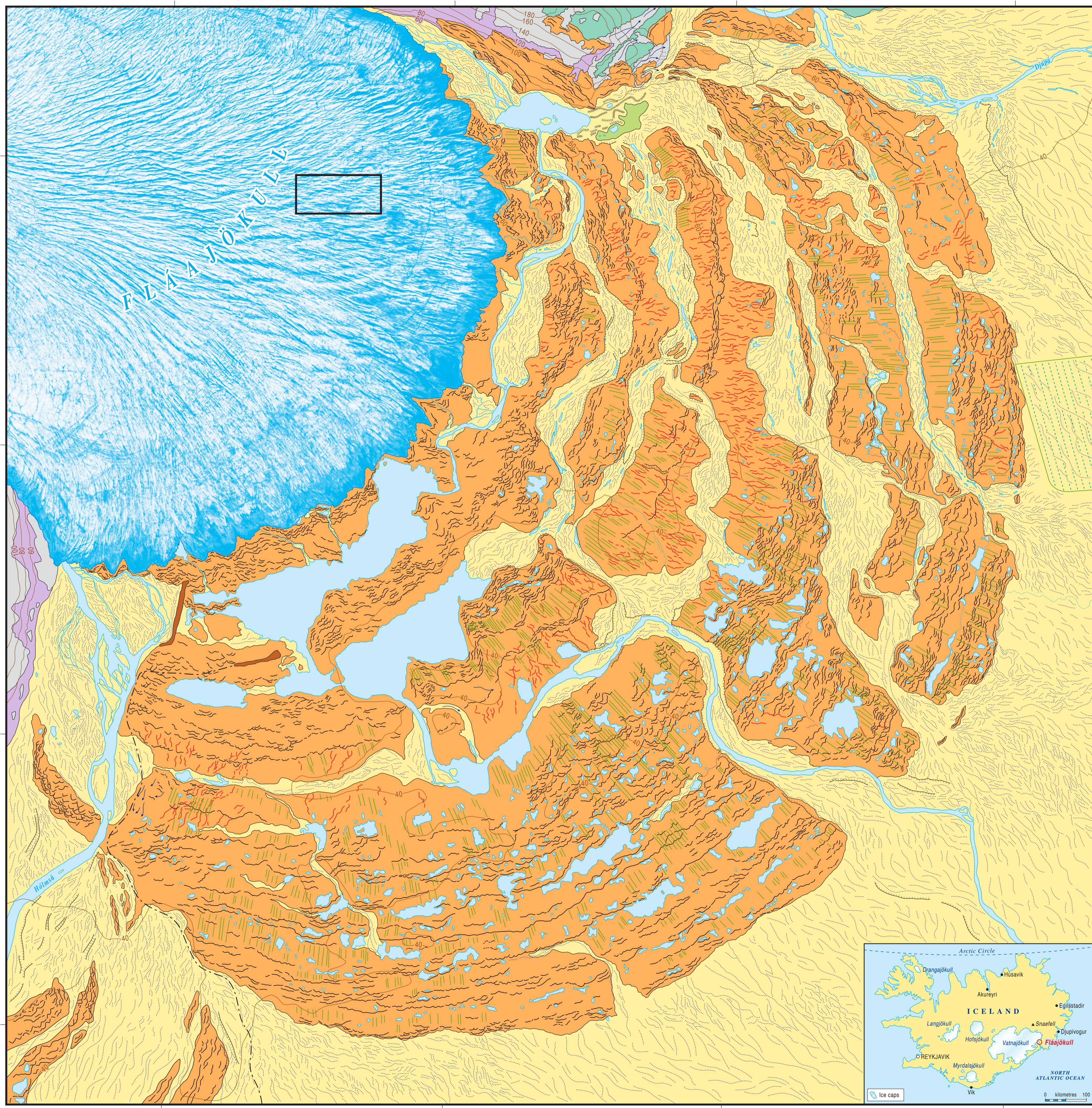
473000

474000

475000

476000

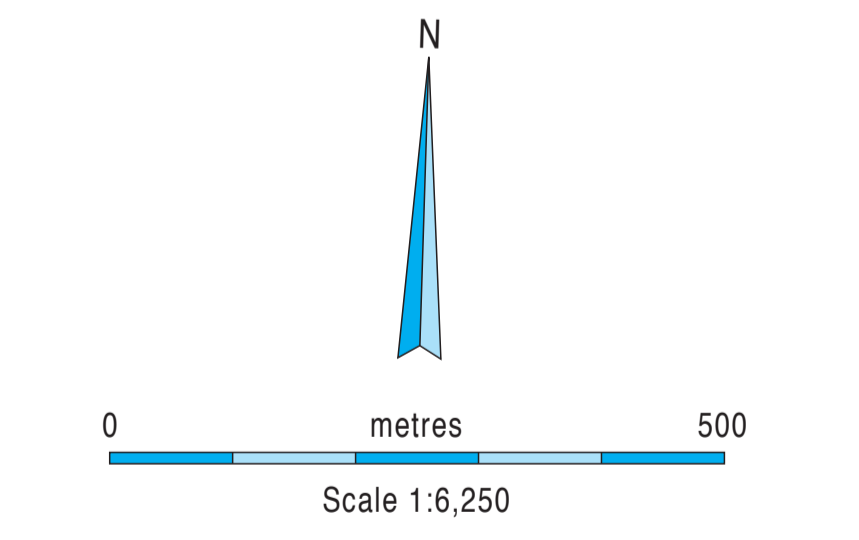
URL: <http://mc.manuscriptcentral.com/tjom>



FLÁAJÖKULL (NORTH LOBE), ICELAND: Active temperate piedmont lobe glacial landsystem

DAVID J.A. EVANS, MAREK EWERTOWSKI
and CHRIS ORTON
Department of Geography, Durham University, UK

- Glacifluvial deposits, including eskers
- Till and moraines dating to the Little Ice Age (superimposed on overridden moraines)
- Residuum or weathered bedrock, and areas of weathered pre-Little Ice Age till (including areas of aeolian deposits and peat)
- Glacilacustrine deposits
- Made ground
- Paraglacial deposits, small bedrock exposures and debris flow fans and scree
- Bedrock (including small patches of residuum and thin till)
- Glacier ice
- Flutings
- Relict channels
- Lakes and kettle holes
- Rivers
- Major terrace
- Meltwater channels
- Esker
- Moraine ridges
- Crevasse fills and minor till eskers
- Contours (20m intervals)
- Track
- Crop patterns
- Field boundaries
- Location of 1:350 scale map



Based on aerial photography by Landmælingar Islands, July 1989.

UTM 28N Projection

Contour interval: 20m
(based on ISN 93 datum)
Lambert Projection

Map to accompany paper:
Evans D.J.A., Ewertowski M and Orton C. (2014)
Fláajökull, Iceland:
Active temperate piedmont lobe glacial landsystem.

© Journal of Maps, 2014.



